

# SIMULATION STUDIES OF PERSISTENT PHOTOCONDUCTIVITY, FILAMENTARY CONDUCTION AND OPTICAL PULSE POSITIONING ON THE HIGH VOLTAGE RESPONSE OF SEMI-INSULATING GaAs PHOTOCONDUCTIVE SWITCHES

R. P. Joshi and P. Kayasit

Dept. of Electrical and Computer Engineering  
Old Dominion University, Norfolk, VA 23529-0246

N. Islam, E. Schamiloglu and C. B. Fleddermann  
Department of Electrical and Computer Engineering  
University of New Mexico, Albuquerque, NM 87131

J. Schoenberg

Air Force Research Laboratory, Kirtland AFB, NM 87117.

**Abstract** : A self-consistent, two-dimensional, time-dependent, drift-diffusion model is developed to simulate the response of high power photoconductive switches. Effects of spatial inhomogeneities associated with the contact barrier potential are shown to foster filamentation. Results of the dark current match available experiments. Persistent photoconductivity is shown to arise at high bias even under conditions of spatial uniformity. Filamentary currents require an inherent spatial inhomogeneity, and are more likely to occur for low optical excitation. Finally, it is shown that the switch response can be varied by changing the spatial position of the optical excitation pulse.

## I. INTRODUCTION

Photoconductive, semiconductor switches (PCSS) based on semi-insulating (SI) GaAs material have been developed in the recent past for pulsed power technology [1-3]. In the non-linear mode at high values of the applied bias, the following features are observed : (A) Photocurrent that scales non-linearly with the incident optical power, making it possible to obtain large circuit currents at *relatively low optical costs*. This implies that an internal mechanism must be at work to create a large supply of mobile charge in the device. (B) The conduction capacity is not limited by the photon flux, and a persistent photoconductivity effect is observed. This indicates an internal mechanism must be maintaining a continuous supply of charge. (C) Finally, the formation of current filaments within the PCSS which lead to overall device failure. Mechanisms such as avalanche ionization [4], field-dependent trap filling [5], double injection [6], recombination radiation [7], and streamer formation [8] have been proposed. Unfortunately, many of the above reports have either analyzed only the steady state conduction characteristics or have used a one dimensional (1D) numerical model. However, such 1D approaches are inadequate for modeling filamentation which inherently is a two-dimensional phenomena. In addition, effects such as current crowding, localized

enhancements of carrier impact ionizations, and evaluations of different device geometries would all be completely overlooked in any 1D study.

The only two-dimensional, time-dependent numerical study on high power PCSS was reported by Stout and Kushner [7]. Recombination radiation and subsequent non-uniform absorption were shown to play an important part in PCSS activated by spatially localized optical excitations. However, an important point worth noting is that filamentary currents and spatially non-uniform carrier densities have been observed in PCSS structures subjected to *uniform* carrier generation [9]. The basic questions regarding the origin, mechanism and dynamics of filament formation under conditions of *uniform* generation remain unresolved.

In this contribution, we include effects of spatial inhomogeneities on the contact characteristics, and simulate the transient response of PCSS devices at high voltages based on a 2D, time-dependent, self-consistent numerical model. The treatment includes barrier height fluctuations, thermionic emission and electron tunneling at the contacts, image barrier lowering (IBL), bulk impact ionization, and trapping/detrapping processes.

## II. BIPOLAR TRANSPORT MODEL

Treatment of bulk semiconductor transport was based on the Drift Diffusion approach. Material parameters for GaAs were taken from the published literature [6], and a list of the values used can be found elsewhere [10]. A sketch of the actual three dimensional (3D) device structure, and its two-dimensional simulation representation is shown in Fig. 1. This structure was based on actual devices grown and tested at the NSWC (Naval Surface Warfare Center) facility.

Salient features of the model include : (i) A Poisson solver. (ii) Time dependent photogeneration with a spatial profile. (iii) Rate equations for transient

## Report Documentation Page

*Form Approved*  
*OMB No. 0704-0188*

Public reporting burden for the collection of information is estimated to average 1 hour per response, including the time for reviewing instructions, searching existing data sources, gathering and maintaining the data needed, and completing and reviewing the collection of information. Send comments regarding this burden estimate or any other aspect of this collection of information, including suggestions for reducing this burden, to Washington Headquarters Services, Directorate for Information Operations and Reports, 1215 Jefferson Davis Highway, Suite 1204, Arlington VA 22202-4302. Respondents should be aware that notwithstanding any other provision of law, no person shall be subject to a penalty for failing to comply with a collection of information if it does not display a currently valid OMB control number.

1. REPORT DATE <b>JUN 1999</b>		2. REPORT TYPE <b>N/A</b>		3. DATES COVERED <b>-</b>	
4. TITLE AND SUBTITLE <b>Simulation Studies Of Persistent Photoconductivity, Filamentary Conduction And Optical Pulse Positioning On The High Voltage Response Of Semi-Insulating GaAs Photoconductive Switches</b>				5a. CONTRACT NUMBER	
				5b. GRANT NUMBER	
				5c. PROGRAM ELEMENT NUMBER	
6. AUTHOR(S)				5d. PROJECT NUMBER	
				5e. TASK NUMBER	
				5f. WORK UNIT NUMBER	
7. PERFORMING ORGANIZATION NAME(S) AND ADDRESS(ES) <b>Dept. of Electrical and Computer Engineering Old Dominion University, Norfolk, VA 23529-0246</b>				8. PERFORMING ORGANIZATION REPORT NUMBER	
9. SPONSORING/MONITORING AGENCY NAME(S) AND ADDRESS(ES)				10. SPONSOR/MONITOR'S ACRONYM(S)	
				11. SPONSOR/MONITOR'S REPORT NUMBER(S)	
12. DISTRIBUTION/AVAILABILITY STATEMENT <b>Approved for public release, distribution unlimited</b>					
13. SUPPLEMENTARY NOTES <b>See also ADM002371. 2013 IEEE Pulsed Power Conference, Digest of Technical Papers 1976-2013, and Abstracts of the 2013 IEEE International Conference on Plasma Science. Held in San Francisco, CA on 16-21 June 2013. U.S. Government or Federal Purpose Rights License.</b>					
14. ABSTRACT <b>A self-consistent, two-dimensional, timedependent, dri%diBusion model is developed to simulate the response of high power photoconductive switches. Effects of spatial inhomogeneities associated with the contact barrier potential are shown to foster filmemation. Results of the dark current match available experiments. Persistent photoconductivity is shown to arise at high bias even under conditions CE spatial uniformity. Filamentary currents require an inherent spatial inhomogeneity, and am more likely to occur for low optical excitation. Finally, it is shown that the switch response can be varied by changing the spatial position of the optical excitation pulse.</b>					
15. SUBJECT TERMS					
16. SECURITY CLASSIFICATION OF:			17. LIMITATION OF ABSTRACT <b>SAR</b>	18. NUMBER OF PAGES <b>5</b>	19a. NAME OF RESPONSIBLE PERSON
a. REPORT <b>unclassified</b>	b. ABSTRACT <b>unclassified</b>	c. THIS PAGE <b>unclassified</b>			

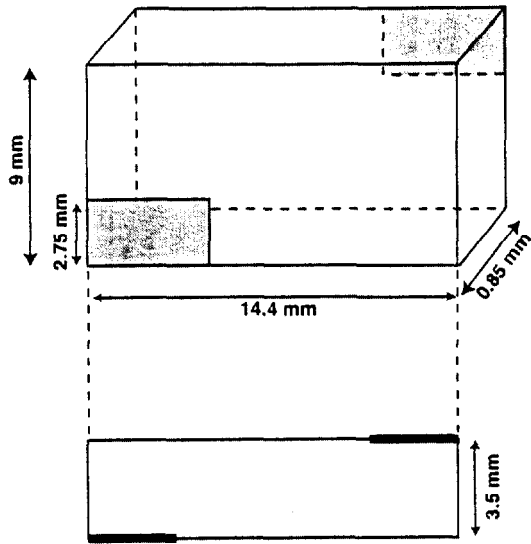


Fig. 1 Sketch of the switch geometry and its assumed for the two dimensional equivalent.

dynamics of the free-carrier generation, trapping and recombination. (iv) A simple external circuit with a 50 Ohm series resistance. (v) Carrier generation through emission from partially filled energy states within the bandgap. (vi) Bulk impact ionization, and contact electron injection by thermionic emission and tunneling. (vii) Barrier height fluctuations leading to spatially non-uniform injection at the contacts. (viii) Uniform discretization into a  $10 \mu\text{m}$  square mesh. (ix) The semiconductor and metal work functions of 4.1 eV and 4.3 eV. (x) The Si-GaAs material was assumed to have an unintentional donor density of  $5 \times 10^{11} \text{ cm}^{-3}$  and a trap concentration of  $5 \times 10^{14} \text{ cm}^{-3}$ . The trap level (assumed to be a donor site) was taken to be 0.3487 eV below the conduction band with electron and hole capture cross sections of  $10^{-15} \text{ cm}^2$  and  $10^{-17} \text{ cm}^2$ , respectively. (xi) An anode barrier height of 0.91 eV. At the cathode, a two-step barrier with values of  $0.91 \pm 0.2 \text{ eV}$  was used to include fluctuations. (xii) Electron injection was considered only at the cathode.

### III. RESULTS AND DISCUSSIONS

Model predictions were first compared against the experimental current-voltage (I-V) measurements conducted at NSWC. The calculated, steady state I-V curves are shown in Fig. 2. The experimental data is also shown, and seen to match the predictions quite well. This validates the present model. In the low to moderate voltage range, the response is nearly linear and displays Ohmic behavior. With increasing bias, a supralinear characteristics is predicted as a result of the negative differential mobility of electrons in GaAs. The overall conduction, therefore, does not change with bias quite as much. Finally, a dramatic increase in the current is predicted near 55 kV. This corresponds to

the on-set of internal impact ionization and the transition to a virtual double injection mode.

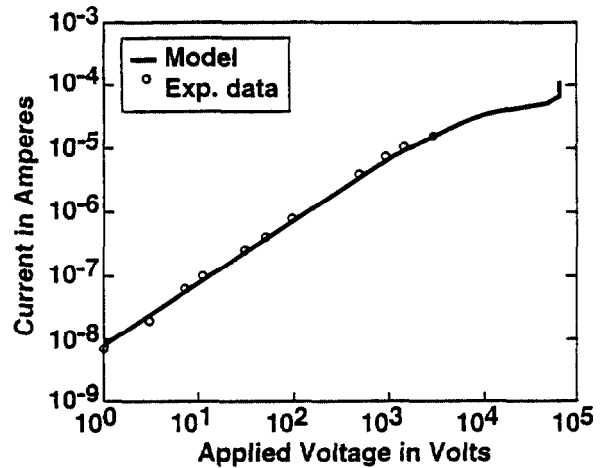


Fig. 2 Comparisons between experimental data and simulation results of the dark current characteristics.

Results of the current transient for a 70 kV bias and a relatively low optical generation function of  $2 \times 10^{24} \text{ m}^{-2} \text{ s}^{-1}$  having a uniform spatial distribution are shown in Fig. 3, with and without barrier height fluctuations. The uniform illumination represents the most ideal situation since any non-uniformity can only add to the potential for instability and filamentation. A

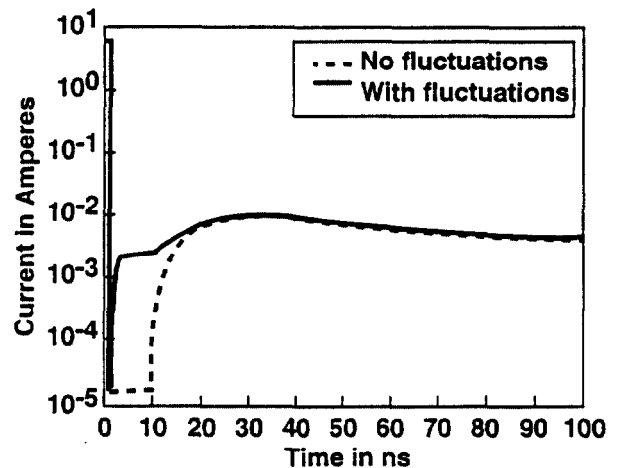


Fig. 3 Simulation results for the PCSS current with and without the barrier height fluctuations.

large displacement current occurs during the first 1 ns due to the voltage ramp. Three features are evident : (A) The dark current is controlled by barrier height fluctuations, and strong current enhancements are predicted with contact inhomogeneity. (B) After

photoexcitation, differences between the two cases become negligible. (C) The photocurrent is predicted to be relatively long lived. This “lock-on” is relatively independent of the contact injection process or details of the barrier height.

A simulation snapshot of the electron density obtained at 100 ns with barrier height fluctuations is shown in Fig. 4. A filamentary structure is clearly evident. The strongest electron conduction occurs between the anode and cathode tips which present the highest electric fields and lowest traversal distance. However, a profile without barrier inhomogeneity in Fig. 5, reveals a total absence of filamentary structures. The values of electron density are also much smaller. The results clearly demonstrate that the presence of non-uniform electric fields alone is insufficient to produce filamentary structure in spite of the impact ionization process. It is thus shown that lock-on does not always imply the existence of filamentary currents.

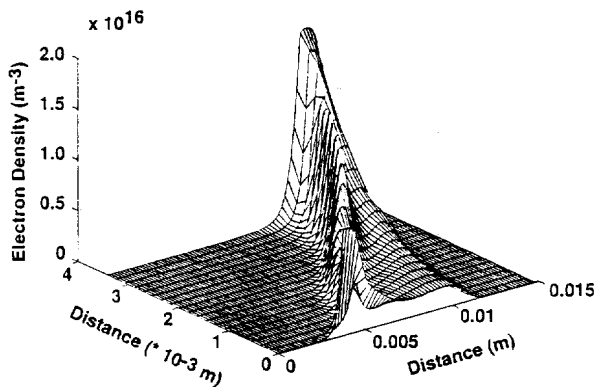


Fig. 4 Results of the internal electron density profile within the PCSS at 100 ns with barrier fluctuations.

Plots of Fig. 6 for a generation of  $2 \times 10^{26} \text{ m}^{-2} \text{ s}^{-1}$  demonstrate the role of impact ionization more clearly. Without ionization, the current exhibits a monotonic decrease towards the dark current value, as the initial population of photogenerated carriers is gradually swept out of the device. With inclusion of the ionization process, the current is seen to be locked-on to a fixed value. Thus it is shown that current lock-on can result following photoexcitation, in keeping with the observed trends in SI GaAs switches. Second, it is localized impact ionization that is potentially responsible. Also, cathode electron injection alone is insufficient to maintain a self-sustaining process.

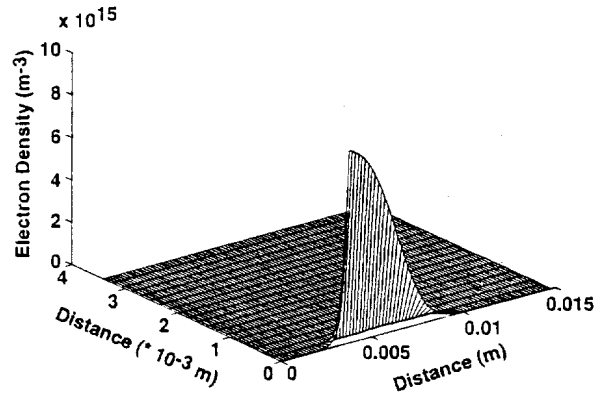


Fig. 5 Snapshot of the electron density distribution at 100 ns in the absence of barrier inhomogeneity.

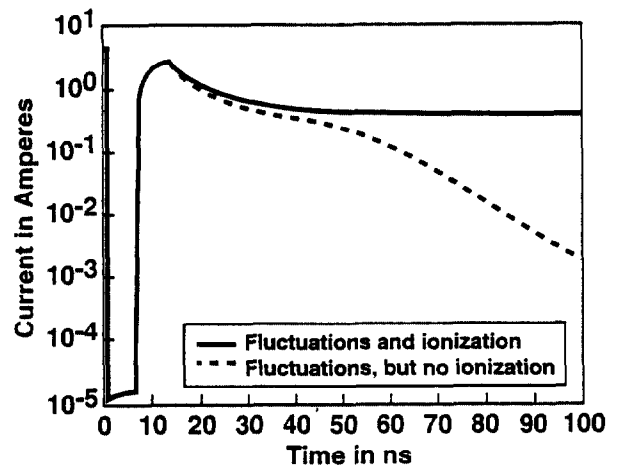


Fig. 6 Device currents with and without bulk impact ionization. Lock-on is predicted only with ionization.

Next, PCSS current results at high optical intensity of  $2 \times 10^{29} \text{ m}^{-2} \text{ s}^{-1}$  with and without barrier fluctuations are shown in Fig. 7. A 5 ns pulse width was chosen, and impact ionization was included. As before, the dark current values are significantly affected by differences in carrier injection at the contacts. However, following photoexcitation, almost identical values are predicted for the two cases. Lock-on into a persistent conductive state is also evident in Fig. 7. Higher carrier generation leads to stronger internal polarization, and electric field enhancements at the contacts. Large electric fields at the contacts serve as localized sources of carrier generation through impact ionization. Hence, the role of carrier injection becomes less important. Second, a virtual injector of electrons at the cathode and holes at the anode is naturally established. This leads to a virtual double injection,

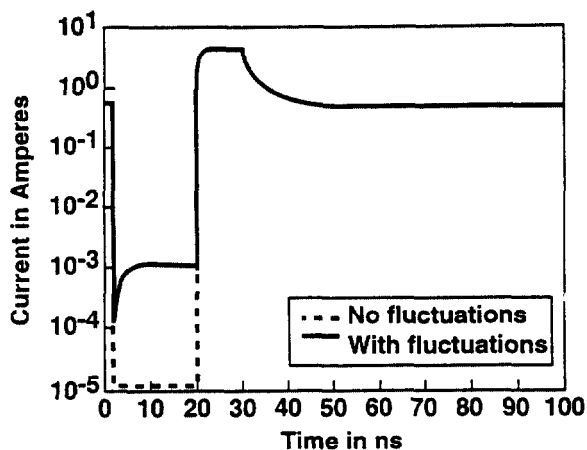


Fig. 7 PCSS currents at higher optical excitation intensities with and without barrier inhomogeneities.

and continued carrier supply for lock-on conductivity.

The electric field distributions  $E_x$  at 50 ns are shown in Fig. 8. The stronger build up at the contacts is evident. Unlike the low optical excitation case, a filamentary mode connecting the two opposed contacts is not predicted here. This suggests that though higher optical excitation would degrade the overall conversion efficiency, it might provide a more stable option.

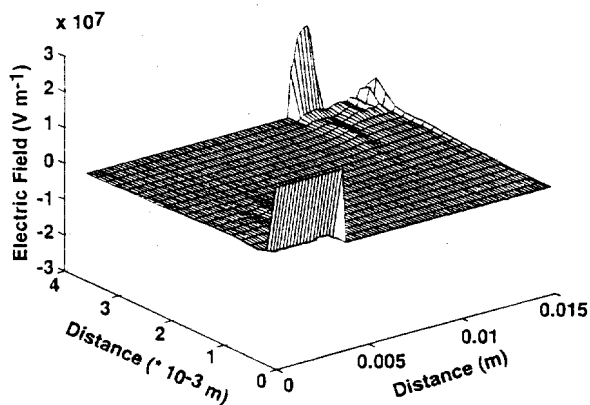


Fig. 8  $E_x$  at 50 ns for high intensity photoexcitation.

Simulations of Figs. 9(a)-(b) show the profiles of the electron and  $E_x$  variables at 20 ns following cathode-side photoexcitation. Electrons created near the cathode drift away, giving rise to a "propagating wave"

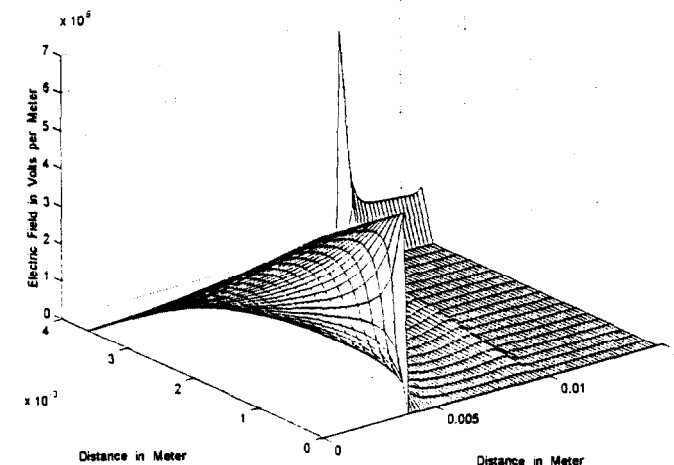
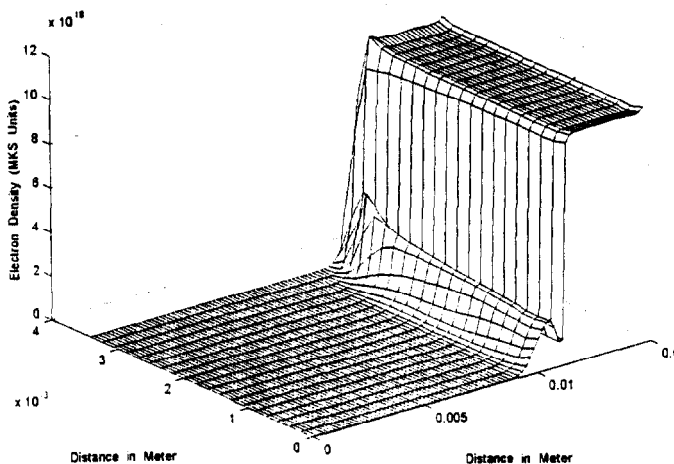


Fig. 9 Profiles at 20 ns for cathode-side laser excitation. (a) Electron density, and (b) the  $E_x$  field.

The electric fields are dramatically *suppressed* over the cathode region due to strong internal polarization. The time dependent current shown in Fig. 10, exhibits no signs of "lock-on". For anode side photogeneration, a long-lived photocurrent is predicted in Fig. 11. This is due to strong electron injection from the cathode where the electric fields tend to be quite high.

#### IV. SUMMARIZING CONCLUSIONS

A self-consistent, 2D, time-dependent, PCSS model

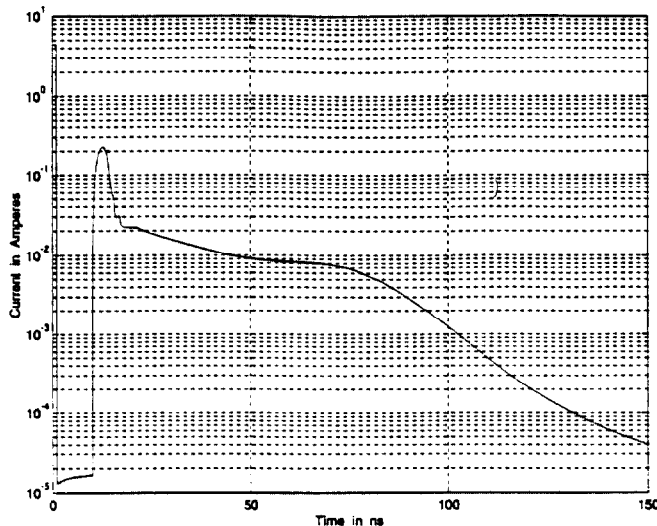


Fig. 10 Current response for cathode-side generation.

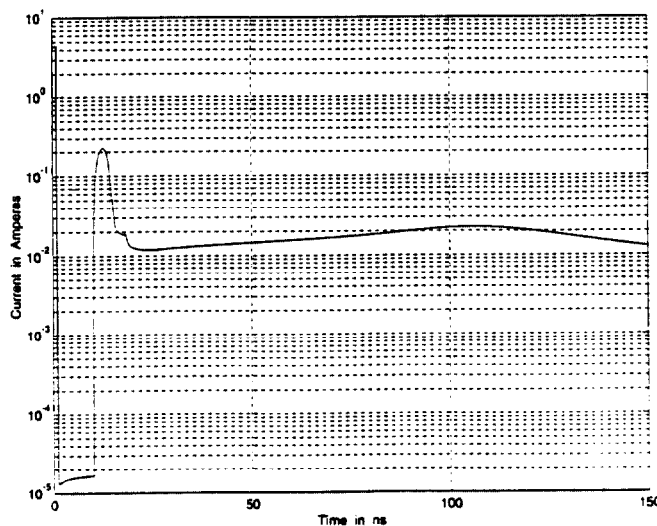


Fig. 11 Time dependent current response for anode-side photogeneration.

has been developed. Results of the dark current matched available experiments. Simulation results demonstrated that lock-on photoconductivity will arise at high applied voltages. It is probably the result of internal impact ionization, and can even exist under

spatially uniform conditions. It was also shown that lock-on and filamentary conduction are distinct phenomena. Filamentary currents require inherent spatial inhomogeneity. Filaments are more likely to occur under conditions of low optical excitation as the internal polarization is insufficient to quench the electric fields. Finally, it was shown that changes in spatial location of the laser pulse can alter the PCSS characteristics. This suggests that high optical excitation or spatial tailoring of the incident pulse profile might provide a simple means of controlling filamentation in high power switches.

*Acknowledgments:* The authors would like to thank D. C. Stoudt and M. Richardson (NSWC) for useful discussions. This work was sponsored in part by the AFOSR under the New World Vistas program.

## V. REFERENCES

1. G. M. Loubriel, F. J. Zutavern, A. Baca, H. P. Hjalmarson, T. A. Plut, W. D. Helgeson, M. O. Malley, and D. J. Brown, *IEEE Trans. Plasma Sci.* **25**, 124 (1997).
2. *High Power Optically Activated Solid-State Switches*, edited by A. Rosen and F. Zutavern (Artech House, Boston, 1994).
3. R. A. Falk, J. Adams, C. D. Capps, S. G. Ferrier, and J. A. Krinsky, *IEEE Trans. Elec. Dev.* **ED-42**, 43 (1995).
4. H. Zhao, P. Hadizad, J. H. Hur, and M. A. Gundersen, *J. Appl. Phys.* **74**, 6645 (1993).
5. W. T. White III, C. G. Dease, M. D. Pocha, and G. H. Khanaka, *IEEE Trans. Elec. Dev.* **ED-37**, 2532 (1990).
6. C. D. Capps, R. A. Falk, and J. C. Adams, *J. Appl. Phys.* **74**, 6645 (1993).
7. P. J. Stoudt and M. Kushner, *J. Appl. Phys.* **79**, 2084 (1996) ; and references therein.
8. J. L. Hudgins, D. W. Bailey, R. A. Dougal, and V. Venkatesan, *IEEE Trans. Power Electronics* **10**, 615 (1995).
9. M. K. Kennedy, R. P. Brinkmann, and K. H. Schoenbach, *IEEE Trans. Electron Devices* **ED-42**, 1009 (1995).
10. R. P. Joshi, P. Kayasit, N. Islam, E. Schamiloglu, C. Fleddermann, and J. Schoenberg, to appear *J. Appl. Phys.*, 1999.